Original Article

Association between the fetal-type posterior cerebral artery and intracranial anterior and posterior circulating atherosclerotic plaques using multi-contrast magnetic resonance vessel wall imaging

Dingqi Liu[1]^, Chenyang Zhao[1], Deng-Ling Zhao[2], Xiao-Hui Chen[2], Dan Zhou[1#], Cheng Li[2#]^

[1]Department of Radiology, BenQ Medical Center, the Affiliated BenQ Hospital of Nanjing Medical University, Nanjing, China; [2]Department of Radiology, Zhongda Hospital, School of Medical, Southeast University, Nanjing, China

Contributions: (I) Conception and design: D Liu; (II) Administrative support: D Zhou, C Li; (III) Provision of study materials or patients: DL Zhao, XH Chen, C Li; (IV) Collection and assembly of data: D Liu; (V) Data analysis and interpretation: D Liu, C Zhao; (VI) Manuscript writing: All authors; (VII) Final approval of manuscript: All authors.

[#]These authors contributed equally to this work and should be considered as co-corresponding authors.

Correspondence to: Dan Zhou, MD. Department of Radiology, BenQ Medical Center, the Affiliated BenQ Hospital of Nanjing Medical University, Jianye District, Nanjing 210000, China. Email: Danny.Zhou@benqmedicalcenter.com; Cheng Li, MD. Department of Radiology, Zhongda Hospital, School of Medical, Southeast University, Gulou District, Nanjing 210009, China. Email: cjr.licheng@vip.163.com.

Background: Intracranial atherosclerotic disease (ICAD) is one of the most common causes of ischemic stroke. The fetal-type posterior cerebral artery (FTP) affects intracranial collateral circulation, which is closely related to the occurrence and development of ICAD. Knowledge of the relationship between FTP and ICAD is important for developing treatment strategies for FTP patients diagnosed with atherosclerotic diseases. This study aims to quantitatively analyze the association between the FTP and intracranial atherosclerotic plaques using magnetic resonance vessel wall imaging (VW-MRI).

Methods: This retrospective study enrolled patients with recent cerebrovascular symptoms (stroke or transient ischemic attack <2 weeks) who were diagnosed with atherosclerotic plaque(s) by VW-MRI in one hospital from October 2018 to March 2022. They were classified into the FTP group and the non-FTP group. Plaque characteristics and vascular-related parameters in intracranial arteries were compared between the two groups. Univariate and multivariate logistic regressions were performed to determine the odds ratios (ORs) and corresponding 95% confidence intervals (CIs) of the plaque characteristics between the two groups.

Results: A total of 104 patients (mean age: 61.8±9.8 years, 57 males) were included for VW-MRI scan analysis. 40 (38.46%) and 64 (61.54%) were classified into the FTP and the non-FTP groups, respectively. The plaques of middle cerebral artery (MCA) in the FTP group were more likely to occur on the dorsal and superior walls of the lumen compared with the non-FTP group (37.50% *vs.* 17.19%, P=0.001). The remodeling index (RI) of MCA was statistically different between the two groups (1.071±0.267 *vs.* 0.886±0.235, P=0.007). No significant differences were found in vertebrobasilar artery (VBA) plaque distributions (17.50% *vs.* 9.38%, 10.00% *vs.* 12.50%, 20.00% *vs.* 17.19%, P>0.05) and characteristics between the two groups (RI: 1.095±0.355 *vs.* 0.978±0.251; eccentricity index: 0.539±1.622 *vs.* 0.550±0.171, P>0.05).

^ ORCID: Dingqi Liu, 0000-0003-3053-6028; Cheng Li, 0000-0003-4804-6027.

Conclusions: The plaques in the FTP group were more likely to occur on the dorsal and superior walls of the MCA, and the presentence of FTP was found to be significantly correlated with vascular remodeling of MCA atherosclerotic plaques. The relationship between the severity of intracranial atherosclerosis and the presence of FTP can provide valuable information for clinicians to intervene early and prevent the occurrence of stroke.

Keywords: Fetal-type posterior cerebral artery (FTP); atherosclerosis; plaque; magnetic resonance vessel wall imaging (VW-MRI)

Submitted May 04, 2023. Accepted for publication Sep 14, 2023. Published online Oct 27, 2023.
doi: 10.21037/qims-23-611
View this article at: https://dx.doi.org/10.21037/qims-23-611

Introduction

Stroke has a high incidence, mortality rate and can lead to different degrees of disability, and has become one of the most important diseases endangering human health (1). Ischemic stroke is one of the stroke types, which accounts for 75–90% of all strokes. The pathogenesis of large-artery atherosclerotic ischemic stroke mainly includes artery-to-artery embolism, hemodynamic damage, and occlusion of penetrating arteries (2). Artery-to-artery embolism is the main cause of the disease. The main source of emboli in ischemic stroke is atherosclerotic high-risk plaque rupture. Therefore, it is important to identify the presence of high-risk plaques at an earlier stage (3,4). In addition to common risk factors such as age, hypertension, diabetes mellitus (DM), and personal lifestyle (5), the pathogenesis of stroke is also related to vascular morphology and intracranial collateral circulation (6,7).

Collaterals are considered to be a predisposition factor for atherosclerotic progression and cerebral infarction (8). Well-developed collateral circulation plays a significant role in maintaining cerebral blood flow. The circle of Willis and the leptomeningeal collaterals are the primary and secondary collateral circulation structures in the brain. The circle of Willis is a communication artery ring of the anterior and posterior circulation. Leptomeningeal collaterals form between the anterior cerebral artery (ACA) and the middle cerebral artery (MCA), the ACA and the posterior cerebral artery (PCA), and the MCA and PCA, bridging the anterior and posterior circulation (9). It mainly plays a role after an ischemic event and when the primary collateral circulation is not adequately compensated (6). Since the ACA and MCA belong to the anterior circulation, and the PCA belongs to the posterior circulation, the collateral circulation between the MCA and the PCA is the most important leptomeningeal collateral circulation in PCA (10). However, only 42–52% of healthy subjects exhibit a configuration of the circle of Willis (11,12). Fetal-type posterior cerebral artery (FTP) is a common structural incomplete variation of the circle of Willis. FTP directly originates from the internal carotid artery and complete FTP (cFTP) is characterized by the absence of the P1 segment, while partial FTP (pFTP) is characterized by hypoplastic of the P1 segment. According to previous studies, it is generally suggested that FTP is present in approximately 11% to 46% of the worldwide population (13,14). When FTP is present, both the PCA and the MCA are supplied by the internal carotid artery, the leptomeningeal collateral circulation formed between the two vessels cannot play the role of communicating between the anterior and posterior circulation. So, the presence of FTP makes it more likely that the cerebral blood supply is inadequate. As one of the configurations of the incomplete circle of Willis, FTP affects intracranial collateral circulation, which is closely related to the occurrence and development of atherosclerotic diseases. Therefore, we hypothesized that FTP may have a certain influence on the occurrence and development of intracranial atherosclerotic diseases (ICADs). The present study aimed to use magnetic resonance vessel wall imaging (VW-MRI) to analyze the association between FTP and the plaques in the intracranial vessels. We present this article in accordance with the STROBE reporting checklist (available at https://qims.amegroups.com/article/view/10.21037/qims-23-611/rc).

Methods

Study population

In this retrospective study, patients with recent cerebrovascular

symptoms (stroke or transient ischemic attack <2 weeks) and intracranial artery atherosclerotic plaques were recruited and diagnosed by VW-MRI in one affiliated university hospital from October 2018 to March 2022. The inclusion criteria were as follows: (I) age ≥18 years; (II) plaques in M1 and M2 segments of the MCA, V4 segment of vertebral artery (VA), and basilar artery (BA) on VW-MRI, which were decided by neuroradiologists. The exclusion criteria were: (I) internal carotid artery stenosis >50%; (II) vasculopathy, including dissection, vasculitis, or moyamoya disease; (III) FTP with contralateral plaques; (IV) cardioembolism and hemorrhagic stroke; (V) other congenital variations in cerebral blood vessels; (VI) history of brain tumor and head and neck surgery; (VII) claustrophobia; and (VIII) contraindication to magnetic resonance imaging (MRI) examination and poor MRI quality. Demographic and clinical information [including age, gender, body mass index (BMI), and a history of smoking, drinking, hypertension, hyperlipidemia, and DM] were collected from clinical records. Hypertension was defined as systolic blood pressure (SBP) ≥140 mmHg or diastolic blood pressure (DBP) ≥90 mmHg. Hyperlipidemia was identified when low-density lipoprotein cholesterol (LDL-C) >1.58 mmol/L, total cholesterol (TC) >2.26 mmol/L, or triglyceride (TG) >1.69 mmol/L. DM was defined as a fasting serum glucose level of >6.9 mmol/L, 2-h post-load glucose level of >11.0 mmol/L, or the use of anti-diabetic medication. The FTP group was defined as those who lacked one or two P1 segment(s) or had a dysplastic P1 segment of PCA, while the non-FTP group was defined as those who had normal P1 segments of PCA. The study was conducted in accordance with the Declaration of Helsinki (as revised in 2013). The study protocol was approved by the ethics committee for Clinical Research of Zhongda Hospital affiliated to Southeast University and all subjects provided written informed consent before participating in the study.

Imaging protocol

The patients who participated in this study underwent carotid and brain MRI on a 3.0T MRI scanner (Philips Ingenia II, Philips Healthcare, Best, The Netherlands) with an 8-channel phased array coil. The MRI protocol included three-dimensional time of flight (3D-TOF), T1-weighted, T2-weighted, and diffusion-weighted imaging (DWI). VW-MRI was performed using non-contrast and post-contrast three-dimensional turbo spin echo (3D T1WI-VISTA) sequences. Before the acquisition of the contrast-enhanced 3D T1WI-VISTA sequence, 0.1 mL/kg of gadolinium contrast agent (0.1 mg/mL; Magnevist; Bayer Schering Pharma AG, Berlin, Germany) was administered to the patient.

3D-TOF magnetic resonance angiography (MRA) was obtained in the axial plane and the scanning parameters were as follows: repetition time/echo time (TR/TE) =15 ms/3.5 ms; flip angle =18°; slice thickness =0.5 mm; matrix size =268 mm × 180 mm; field of view (FOV) =200 mm × 200 mm; voxel =0.75×0.75×0.75; the number of average (NEX) =1; 3D-TOF MRA scan time of 4 min.

Non-contrast and post-contrast VW-MRI were obtained on the coronal plane. The 3D VISTA sequence was used to inhibit the blood flow and optimize the display of the intracranial vascular wall. The scanning parameters were as follows: TR/TE =800 ms/16 ms; flip angle =90°; slice thickness =0.5 mm; matrix size =400 mm × 400 mm; FOV =200 mm × 200 mm; voxel =0.5×0.5×0.5; the NEX =1; the VW-MRI scan time was 5 min and 28 s.

Imaging analysis

The morphological evaluation of the plaque and the measurement of the vessels were performed on the custom-designed software of CASCADE (University of Washington, Seattle, WA, USA). A 4-point scale (1= poor and 4= excellent) was adopted according to the sharpness and contrast between the vessel wall and the surrounding fat tissues to assess the image quality for each slice; images with quality scores <2 were excluded from the study. Maximal lumen narrowing (MLN) was selected for the lesion slice and the normal vessels at the proximal or distal end of the lesion were selected as the referential lumen (RL). The regions of interest (ROIs) were manually drawn to calculate the cross-sectional area of the vessel, including lumen area (LA), vessel area (VA), maximal wall thickness (WTmax), and minimal wall thickness (WTmin). The ROIs for each measurement were drawn twice by two neuroradiologists who had more than 2 years of experience. The average of the measurements of the two neuroradiologists was obtained as the final result. The quantitative calculation of the pertinent parameters was performed as follows: (I) luminal stenosis = $(1 - LA_{MLN}/LA_{RL}) \times 100\%$; (II) the RI = VA_{MLN}/VA_{RL}, RI ≥1.05 was defined as positive remodeling, RI ≤0.95 was defined as negative remodeling, RI between 0.95 and 1.05 was defined as non-remodeling (15). (III) Eccentricity degree = $(WT_{max} - WT_{min})/WT_{max}$. The eccentric plaque was defined as eccentricity degree ≥0.5,

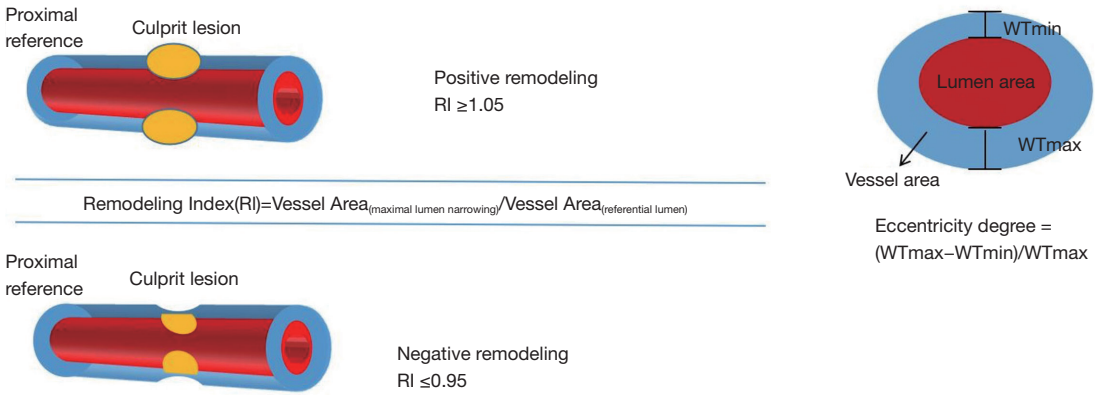

Figure 1 Diagram of the remodeling index and eccentricity degree. Blue: vessel. Red: lumen. Yellow: culprit lesion. RI, remodeling index; WT, wall thickness.

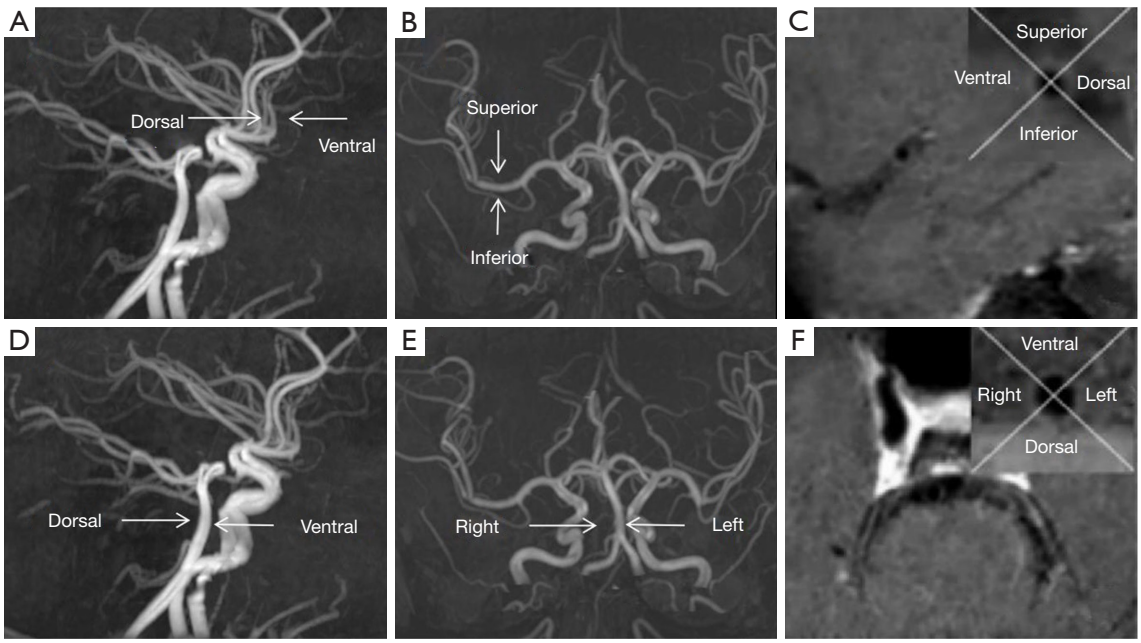

Figure 2 Plaque location diagram. (A-C) The wall of MCA was divided into superior, inferior, ventral and dorsal walls. (D-F) The VBA vessel wall was divided into left, right, ventral and dorsal walls. MCA, middle cerebral artery; VBA, vertebrobasilar artery.

whereas the concentric plaque was defined as eccentricity <0.5 (*Figure 1*).

The plaque distribution at the narrowest lumen was evaluated by dividing the cross-section into four equal arcs on the T1WI enhancement images. The center of the grid was placed at the geometric center of the lumen. The quadrant where the thickest part of the lumen wall was located was the location of the plaque. MCA plaque was divided into ventral, superior, dorsal, and inferior, and vertebrobasilar artery (VBA) plaque was divided into ventral, dorsal, left, and right (16) (*Figure 2*).

Degree of plaque enhancement: (I) no enhancement: the degree of enhancement was similar to or less than that of the normal intracranial arterial wall; (II) enhancement: the degree of enhancement was greater than that of the normal intracranial arterial wall (17).

Statistical analysis

All data were analyzed using SPSS 25.0 software (IBM Corp., Armonk, NY, USA). The continuous variables were expressed as mean ± standard deviation. The categorical variables were presented as percentages. Categorical variables were compared using Pearson's chi-squared test or Fisher's exact probability test (if ≤20% of the expected cell counts were <5). The *t*-test was used for the analysis of the continuous variables with normal distribution and Wilcoxon's signed-rank test was used for the analysis of the continuous variables with abnormal distribution. Univariate and multivariate logistic regressions were performed to determine the odds ratios (ORs) and corresponding 95% confidence intervals (CIs) of the plaque characteristics between the FTP and the non-FTP groups, whereas the clinical characteristics of the study population were also taken into account. A P<0.05 (2-sided) was considered to indicate a statistically significant difference.

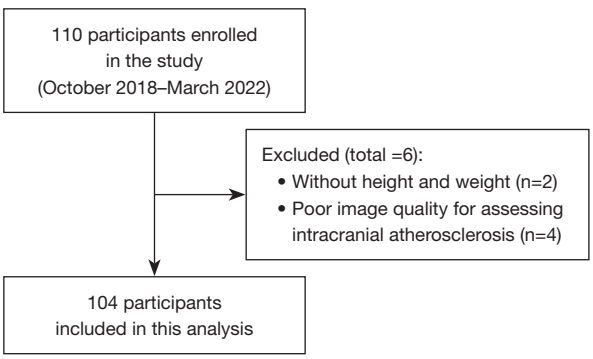

Figure 3 Flow chart of the participant selection.

Results

Clinical characteristics of the study population

A total of 110 patients who met the inclusion criteria were finally enrolled and 6 patients were excluded due to a lack of clinical information or poor image quality. The process of patient selection is shown in *Figure 3*. Of the remaining 104 subjects (mean age: 61.8±9.8 years; 57 males and 47 females), we classified them into the FTP group (n=40) and the non-FTP group (n=64). There were significant differences in DM between the two groups (P<0.05), the FTP group had a higher rate of diabetic patients, but there was no statistical significance in other variables, including age, gender, BMI, clinical risk factors of smoking, drinking, hypertension, and hyperlipidemia (all P values >0.05) (*Table 1*).

Plaque distribution

In MCA atherosclerotic plaques, the FTP group had 6 plaques on the ventral and inferior walls and 15 plaques on the dorsal and superior walls. In the non-FTP group, there were 28 plaques on the ventral and inferior walls and 11 plaques on the dorsal and superior walls. Plaques in the FTP group were more likely to be located on the dorsal and superior wall of the MCA, while plaques in the non-FTP group were more likely to be located on the ventral and inferior wall, with a statistically significant difference in plaque distribution between the two groups (P=0.001).

Among the VBA atherosclerosis plaques in the FTP group, there were 7 plaques on the ventral wall, 4 on the dorsal wall, 4 on the left wall, and 4 on the right wall. In

Table 1 Characteristics of the study patients (n=104)

Characteristics	FTP group (n=40)	Non-FTP group (n=64)	P value
Age (years)	63.500±7.428	60.690±10.893	0.268
Male	20 (50.00)	37 (57.81)	0.436
Body mass index (kg/m^2)	25.068±3.660	24.353±3.015	0.920
Smoking	7 (17.50)	19 (29.69)	0.163
Drinking	6 (15.00)	13 (20.31)	0.495
Hypertension	27 (67.50)	48 (75.00)	0.407
Hyperlipidemia	5 (12.50)	6 (9.38)	0.614
Diabetes mellitus	25 (62.50)	20 (31.25)	0.002*

Data are presented as mean ± standard deviation or n (%). *, statistically significant. FTP, fetal-type posterior cerebral artery.

Table 2 Distribution of plaques

Vessels	Distribution	FTP group (n=40)	Non-FTP group (n=64)	P value
MCA	Ventral and inferior wall	6 (15.00)	28 (43.75)	0.001*
	Dorsal and superior wall	15 (37.50)	11 (17.19)	
VBA	Ventral wall	7 (17.50)	6 (9.38)	0.581
	Dorsal wall	4 (10.00)	8 (12.50)	
	Bilateral walls	8 (20.00)	11 (17.19)	

Data are presented as n (%). *, statistically significant. FTP, fetal-type posterior cerebral artery; MCA, middle cerebral artery; VBA, vertebrobasilar artery.

Table 3 Morphological features of the MCA plaque

Plaque features	FTP group (n=21)	Non-FTP group (n=39)	P value
LA_{MLN} (mm^2)	0.922±0.686	0.885±0.535	0.647
VA_{MLN} (mm^2)	8.941±3.061	9.049±2.761	0.994
Luminal stenosis (%)	46±25	56±23	0.180
Remodeling index	1.071±0.267	0.886±0.235	0.007*
Positive remodeling	10 (47.62)	9 (23.08)	0.051
Negative remodeling	4 (19.05)	20 (51.28)	0.015*
Eccentricity degree	0.610±0.182	0.594±0.229	0.788
Eccentric plaque	14 (66.67)	28 (71.79)	0.679
Enhancement	18 (85.71)	22 (56.41)	0.022*

Data are presented as mean ± standard deviation or n (%). *, statistically significant. MCA, middle cerebral artery; FTP, fetal-type posterior cerebral artery; LA_{MLN}, lumen area (maximal lumen narrowing); VA_{MLN}, vessel area (maximal lumen narrowing).

the non-FTP group, there were 6 plaques on the ventral wall, 8 plaques on the dorsal wall, 6 plaques on the left wall, and 5 plaques on the right wall. Plaques in the FTP group were more likely to be located on the ventral wall, while those in the non-FTP group were more likely to be located on the dorsal wall. There was no significant difference in plaque distribution between the two groups (P=0.581) (*Table 2*).

Differences in plaque characteristics of MCA and VBA between the two groups

In MCA, the difference in vascular remodeling and plaque enhancement between the two groups was statistically significant (P<0.05). Positive remodeling of the MCA was observed in 47.62% of the FTP group and negative remodeling of the MCA was observed in 51.28% of the non-FTP group. The FTP group had more enhanced plaques (85.71% *vs.* 56.41%, P=0.022) compared with those of the non-FTP group. No significant differences were noted in the characteristics of the VBA plaques between the two groups (P>0.05 for all comparisons, as shown in *Tables 3*,*4*). The representative images indicating the different plaque features in the two groups are shown in *Figures 4*,*5*.

Logistic regression analysis of MCA plaque characteristics between the two groups

Univariate logistic regression analysis indicated that the RI of MCA was associated with FTP (OR =24.973; 95% CI: 1.923–324.302, P=0.014). After adjusted for age, gender, hypertension, DM, BMI, and luminal stenosis, the RI of MCA indicated significant differences between the FTP and the non-FTP groups (OR =30.125; 95% CI: 1.262–719.079;

Table 4 Morphological features of the VBA plaques

Plaque features	FTP group (n=19)	Non-FTP group (n=25)	P value
LA_{MLN} (mm^2)	1.948±1.943	1.801±1.499	0.906
VA_{MLN} (mm^2)	15.217±4.963	17.971±7.641	0.156
Luminal stenosis (%)	39±18	42±22	0.697
Remodeling index	1.095±0.355	0.978±0.251	0.337
Positive remodeling	8 (42.11)	8 (32.00)	0.490
Negative remodeling	8 (42.11)	13 (52.00)	0.515
Eccentricity degree	0.539±1.622	0.550±0.171	0.836
Eccentric plaque	13 (68.42)	14 (56.00)	0.402
Enhancement	17 (89.47)	19 (76.00)	0.433

Data are presented as mean ± standard deviation or n (%). *, statistically significant. VBA, vertebrobasilar artery; FTP, fetal-type posterior cerebral artery; LA_{MLN}, lumen area (maximal lumen narrowing); VA_{MLN}, vessel area (maximal lumen narrowing).

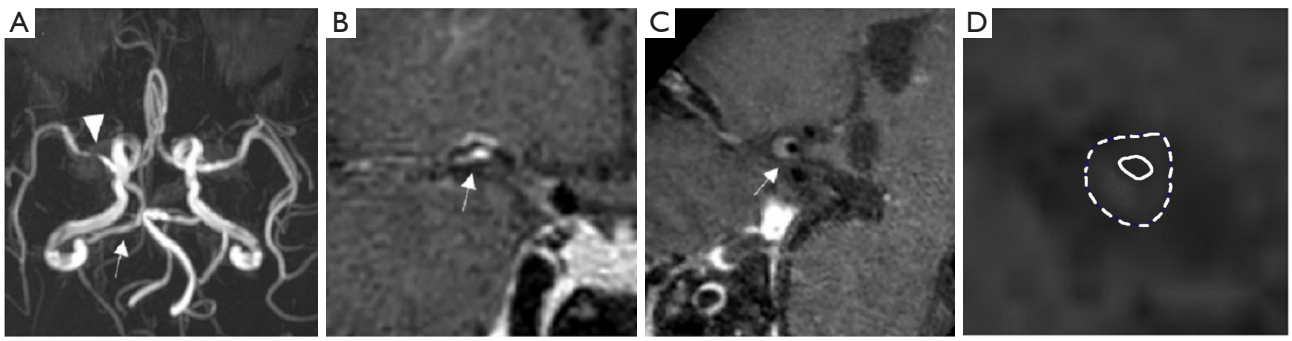

Figure 4 Images of a 52-year-old male patient with FTP. (A) The TOF-MRA manifests stenosis of the M1 segment of the right MCA (arrowhead). The presence of FTP is shown (arrow). (B) The coronary T1-weighted VW-MRI demonstrates an enhanced plaque in the M1 segment of the right MCA (arrow). (C) The transverse T1-weighted VW-MRI indicates the presence of eccentric plaque (arrow). (D) Measurement at the most narrowed site in the T1-weighted VW-MRI: the vessel area was 5.61 mm^2 (dotted white circle) and the lumen area was 1.12 mm^2 (solid white circle). The remodeling index was calculated as follows: remodeling index = 1.17 (positive remodeling). FTP, fetal-type posterior cerebral artery; TOF, time of flight; MRA, magnetic resonance angiography; MCA, middle cerebral artery; VW-MRI, magnetic resonance vessel wall imaging.

P=0.035) (*Table 5*).

Discussion

Vascular remodeling

According to a previous study, the formation of FTP is not related to congenital genetic factors nor acquired neck activity (18). Instead, it is mainly related to the changes noted in cerebral hemodynamics (19). The internal carotid artery in the FTP supplies both PCA and MCA. The additional presence of the tentorium cerebellum affects the anterior and posterior circulation of the leptomeningeal collateral circulation (9,20). These hemodynamic changes play an important role in the development of atherosclerosis (21-24). In this study, the RI of MCA and VBA showed that the MCA plaques in the FTP group were more prone to positive remodeling than that in the non-FTP group, while the RI of VBA showed no significant statistical difference. This is consistent with the results of Lambert *et al.*, Hong *et al.* (25,26). Hong *et al.* reported that the presence of the

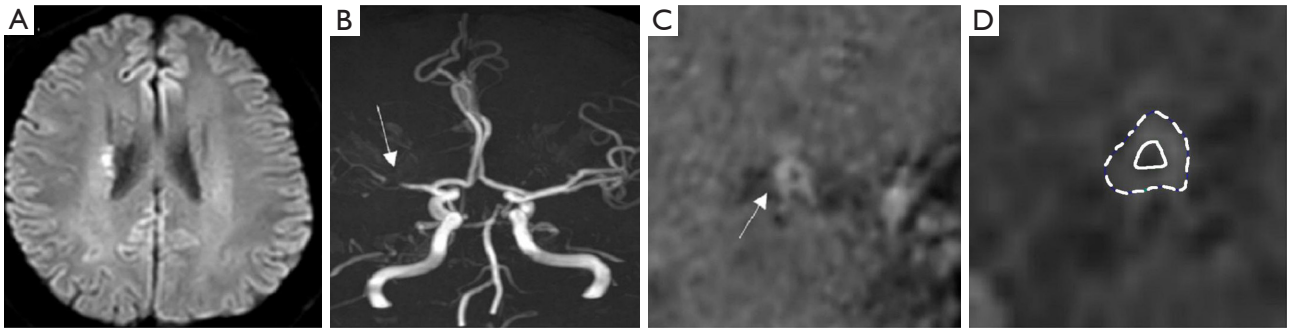

Figure 5 Images of a 53-year-old male patient without FTP. (A) DWI indicates an acute ischemic stroke in the distribution of the right MCA. (B) The TOF-MRA manifests severe stenosis of the M1 segment of the right MCA (arrow). (C) The transverse T1-weighted VW-MRI demonstrates a plaque in the M1 segment of the right MCA (arrow). (D) Measurement at the most narrowed site in the T1-weighted VW-MRI: the vessel area was 7.43 mm^2 (dotted white circle) and the lumen area was 0.4 mm^2 (solid white circle). The remodeling index was calculated as follows: remodeling index =0.53 (negative remodeling). FTP, fetal-type posterior cerebral artery; DWI, diffusion-weighted imaging; MCA, middle cerebral artery; TOF, time of flight; MRA, magnetic resonance angiography; VW-MRI, magnetic resonance vessel wall imaging.

Table 5 Univariate and multivariate logistic regression analyses

Variables	FTP group *vs.* non-FTP group					
	Univariate regression			Multivariate regression[†]		
	OR	95% CI	P value	OR	95% CI	P value
Age	1.048	0.993–1.106	0.090	1.055	0.986–1.129	0.122
Male	0.522	0.178–1.528	0.235	0.217	0.044–1.083	0.062
Hypertension	0.690	0.217–2.194	0.529	0.214	0.033–1.368	0.103
Diabetes mellitus	2.314	0.767–6.983	0.137	3.044	0.746–12.410	0.121
Body mass index	1.021	0.848–1.228	0.828	1.042	0.832–1.306	0.719
Luminal stenosis	0.163	0.016–1.602	0.120	0.219	0.013–3.606	0.288
Remodeling index	24.973	1.923–324.302	0.014*	30.125	1.262–719.079	0.035*

[†], adjusted for age, gender, hypertension, diabetes mellitus, body mass index, and luminal stenosis; *, statistically significant. FTP, fetal-type posterior cerebral artery; CI, confidence interval; OR, odds ratio.

FTP could increase the compensatory blood flow of the internal carotid artery system and reduce the vertebrobasilar blood flow (26), resulting in vascular dilation and reduced blood flow rate in MCA. Lu *et al.* demonstrated that the low blood flow rate could decrease wall shear stress (WSS) (27). Persistent low WSS promoted early plaque growth (27,28). Atherosclerotic arteries exposed to low WSS exhibit uncontrolled inflammation and matrix degradation, leading to lumen enlargement and increased plaque size, further reducing WSS and leading to endothelial dysfunction, known as pathological remodeling. This response may be an attempt by the plaque to maintain luminal morphology during early growth, but it may also be a result of a vicious cycle, leading to expanding plaques and positive remodeling of the lumen (28). This is the reason why positive remodeling is a crucial mechanism of atherosclerotic plaque formation. In advanced atherosclerosis, once positive remodeling is restricted, plaque growth further invades the lumen. This results in an elevated WSS proximal to the lesion and a persistent decrease in the distal WSS. High WSS induces endothelial cell apoptosis and a reduction in endothelial cell contact with the underlying extracellular

matrix, leading to plaque rupture or plaque erosion, and thus promoting the development of atherosclerotic plaques. This may be consistent with the development of plaque vulnerabilities such as lipid-rich necrotic core and thin fibrous caps (29). Under the effect of blood flow impact force, plaques are easy to be damaged and detached, and block downstream small branch vessels, which is more likely to cause acute ischemic stroke (30-32).

Plaque distribution and enhancement

Several studies have demonstrated that small branches of the MCA are mostly located on the dorsal and superior wall of the lumen, the plaque distributed on the superior and dorsal wall of the lumen is easy to block the small branches of the MCA such as the lenticulostriate arteries or extend into the perforating arteries, leading to the occurrence of ischemic stroke (17,33,34). VBA plaques tend to be located on the dorsal and bilateral walls, which are more prone to ischemic events and different from the distribution pattern of atherosclerotic plaques in coronary arteries and MCA (35,36). In our study, the plaques of the FTP group were more prone to be located on the dorsal and superior wall in MCA, which was the same as the research results of scholars, and also indicated that the MCA plaques in the FTP group were more likely to block the perforating artery and cause acute cerebral infarction. However, there was no significant difference in the distribution location of VBA plaque between the two groups.

Plaque enhancement is one of the common signs of vulnerable plaques, and the mechanism of enhancement may be associated with vessel wall neovascularization, inflammation, and increased permeability of endothelial cells (37). The enhancement of intracranial atherosclerotic plaque is closely related to recent cerebral ischemia events (38). Studies have shown that plaque enhancement is an independent risk factor for recurrent stroke (39-42). In the study, the FTP group had more enhanced plaques than the non-FTP group in MCA, which also showed that MCA plaques in the FTP group were more likely to cause acute cerebral infarction. As previously mentioned, the presence of the FTP could result in vascular dilation in MCA, and BA diameter to become smaller (43). The study found that the positive remodeling group was easy to form plaques with a large load and had more significantly enhanced plaques than the non-positive remodeling group, which may indicate a higher degree of inflammation in positive remodeling plaques (30). Larger plaques have a relatively larger lipid-rich necrotic core, and as the necrotic core progresses, neovascularization increases and the plaque ruptures (44). At the same time, the positive remodeling vessel wall bears greater WSS (45), high WSS will prompt plaque rupture or plaque erosion (46), so it is more likely to cause MCA plaque enhancements.

Limitation

The present study is one of the first studies that focus on the difference between anterior and posterior cerebral circulating artery plaques caused by FTP. By contrast, most of the previous studies focused on ischemic stroke due to changes occurring in the intracranial collateral circulation caused by FTP. Despite its novelty, the present study exhibits several limitations. Firstly, the sample size was small, and a single-center study design was used. Certain patients could not be included due to incomplete clinical data. Secondly, data processing was performed by an independent investigator and not by software, which may be subject to selective bias. Thirdly, due to low image resolution, the components of the intracranial arterial plaques were not studied.

Conclusions

The present study suggests that the plaques in the FTP group were more likely to occur on the dorsal and superior walls of the MCA, and the presentence of FTP was found to be significantly correlated with vascular remodeling of MCA atherosclerotic plaques.

Acknowledgments

Funding: This study was supported by the program of the Jiangsu Provincial Commission of Health and Family Planning of China (No. H2017008 and No. M2020041), the Natural Science Foundation of Jiangsu Province (No. BK20170704).

Footnote

Reporting Checklist: The authors have completed the STROBE reporting checklist. Available at https://qims.amegroups.com/article/view/10.21037/qims-23-611/rc

Conflicts of Interest: All authors have completed the ICMJE uniform disclosure form (available at https://qims.

amegroups.com/article/view/10.21037/qims-23-611/coif). The authors have no conflicts of interest to declare.

Ethical Statement: The authors are accountable for all aspects of the work in ensuring that questions related to the accuracy or integrity of any part of the work are appropriately investigated and resolved. The study was conducted in accordance with the Declaration of Helsinki (as revised in 2013). The study protocol was approved by the ethics committee for Clinical Research of Zhongda Hospital affiliated to Southeast University and all subjects provided written informed consent before participating in the study.

References

1. Benjamin EJ, Muntner P, Alonso A, Bittencourt MS, Callaway CW, Carson AP, et al. Heart Disease and Stroke Statistics-2019 Update: A Report From the American Heart Association. Circulation 2019;139:e56-528.
2. Zou XD, Chung YC, Zhang L, Han Y, Yang Q, Jia J. Middle Cerebral Artery Atherosclerotic Plaques in Recent Small Subcortical Infarction: A Three-Dimensional High-resolution MR Study. Biomed Res Int 2015;2015:540217.
3. Qureshi AI, Caplan LR. Intracranial atherosclerosis. Lancet 2014;383:984-98.
4. Xu WH, Li ML, Gao S, Ni J, Zhou LX, Yao M, Peng B, Feng F, Jin ZY, Cui LY. In vivo high-resolution MR imaging of symptomatic and asymptomatic middle cerebral artery atherosclerotic stenosis. Atherosclerosis 2010;212:507-11.
5. Lindenholz A, van der Kolk AG, van der Schaaf IC, van der Worp HB, Harteveld AA, Dieleman N, Bots ML, Hendrikse J. Intracranial Atherosclerosis Assessed with 7-T MRI: Evaluation of Patients with Ischemic Stroke or Transient Ischemic Attack. Radiology 2020;295:162-70.
6. Wufuer A, Mijiti P, Abudusalamu R, Dengfeng H, Jian C, Jianhua M, Xiaoning Z. Blood pressure and collateral circulation in acute ischemic stroke. Herz 2019;44:455-9.
7. Leng X, Lan L, Liu L, Leung TW, Wong KS. Good collateral circulation predicts favorable outcomes in intravenous thrombolysis: a systematic review and meta-analysis. Eur J Neurol 2016;23:1738-49.
8. Yang M, Ma N, Liu L, Wang A, Jing J, Hou Z, Liu Y, Lou X, Miao Z, Wang Y. Intracranial collaterals and arterial wall features in severe symptomatic vertebrobasilar stenosis. Neurol Res 2020;42:649-56.
9. Brozici M, van der Zwan A, Hillen B. Anatomy and functionality of leptomeningeal anastomoses: a review. Stroke 2003;34:2750-62.
10. Arat A, Islak C, Saatci I, Kocer N, Cekirge S. Endovascular parent artery occlusion in large-giant or fusiform distal posterior cerebral artery aneurysms. Neuroradiology 2002;44:700-5.
11. Krabbe-Hartkamp MJ, van der Grond J, de Leeuw FE, de Groot JC, Algra A, Hillen B, Breteler MM, Mali WP. Circle of Willis: morphologic variation on three-dimensional time-of-flight MR angiograms. Radiology 1998;207:103-11.
12. Alpers BJ, Berry RG, Paddison RM. Anatomical studies of the circle of Willis in normal brain. AMA Arch Neurol Psychiatry 1959;81:409-18.
13. De Silva KR, Silva TR, Gunasekera WS, Jayesekera RW. Variation in the origin of the posterior cerebral artery in adult Sri Lankans. Neurol India 2009;57:46-9.
14. Saeki N, Rhoton AL Jr. Microsurgical anatomy of the upper basilar artery and the posterior circle of Willis. J Neurosurg 1977;46:563-78.
15. Qiao Y, Anwar Z, Intrapiromkul J, Liu L, Zeiler SR, Leigh R, Zhang Y, Guallar E, Wasserman BA. Patterns and Implications of Intracranial Arterial Remodeling in Stroke Patients. Stroke 2016;47:434-40.
16. Huang B, Yang WQ, Liu XT, Liu HJ, Li PJ, Lu HK. Basilar artery atherosclerotic plaques distribution in symptomatic patients: a 3.0T high-resolution MRI study. Eur J Radiol 2013;82:e199-203.
17. Lu SS, Ge S, Su CQ, Xie J, Shi HB, Hong XN. Plaque Distribution and Characteristics in Low-Grade Middle Cerebral Artery Stenosis and Its Clinical Relevance: A 3-Dimensional High-Resolution Magnetic Resonance Imaging Study. J Stroke Cerebrovasc Dis 2018;27:2243-9.
18. Schomer DF, Marks MP, Steinberg GK, Johnstone IM, Boothroyd DB, Ross MR, Pelc NJ, Enzmann DR. The anatomy of the posterior communicating artery as a risk factor for ischemic cerebral infarction. N Engl J Med 1994;330:1565-70.

19. Van Overbeeke JJ, Hillen B, Tulleken CA. A comparative study of the circle of Willis in fetal and adult life. The configuration of the posterior bifurcation of the posterior communicating artery. J Anat 1991;176:45-54.
20. van Raamt AF, Mali WP, van Laar PJ, van der Graaf Y. The fetal variant of the circle of Willis and its influence on the cerebral collateral circulation. Cerebrovasc Dis 2006;22:217-24.
21. Davies PF, Tripathi SC. Mechanical stress mechanisms and the cell. An endothelial paradigm. Circ Res 1993;72:239-45.
22. Weinbaum S, Chien S. Lipid transport aspects of atherogenesis. J Biomech Eng 1993;115:602-10.
23. Fung YC, Liu SQ. Elementary mechanics of the endothelium of blood vessels. J Biomech Eng 1993;115:1-12.
24. Schmid-Schoenbein GW, Fung YC, Zweifach BW. Vascular endothelium-leukocyte interaction; sticking shear force in venules. Circ Res 1975;36:173-84.
25. Lambert SL, Williams FJ, Oganisyan ZZ, Branch LA, Mader EC Jr. Fetal-Type Variants of the Posterior Cerebral Artery and Concurrent Infarction in the Major Arterial Territories of the Cerebral Hemisphere. J Investig Med High Impact Case Rep 2016;4:2324709616665409.
26. Hong JM, Lee JS, Shin DH, Yong SW. Hemodynamic impact of fetal-variant Willisian circle on cerebral circulation: a duplex ultrasonography study. Eur Neurol 2011;65:340-5.
27. Lu S, Zhang S. Atherosclerosis research: the impact of physiological parameters on vascular wall stress. SN Appl Sci 2019;1:692.
28. Corban MT, Eshtehardi P, Suo J, McDaniel MC, Timmins LH, Rassoul-Arzrumly E, Maynard C, Mekonnen G, King S 3rd, Quyyumi AA, Giddens DP, Samady H. Combination of plaque burden, wall shear stress, and plaque phenotype has incremental value for prediction of coronary atherosclerotic plaque progression and vulnerability. Atherosclerosis 2014;232:271-6.
29. Chatzizisis YS, Baker AB, Sukhova GK, Koskinas KC, Papafaklis MI, Beigel R, Jonas M, Coskun AU, Stone BV, Maynard C, Shi GP, Libby P, Feldman CL, Edelman ER, Stone PH. Augmented expression and activity of extracellular matrix-degrading enzymes in regions of low endothelial shear stress colocalize with coronary atheromata with thin fibrous caps in pigs. Circulation 2011;123:621-30.
30. Zhang DF, Chen YC, Chen H, Zhang WD, Sun J, Mao CN, Su W, Wang P, Yin X. A High-Resolution MRI Study of Relationship between Remodeling Patterns and Ischemic Stroke in Patients with Atherosclerotic Middle Cerebral Artery Stenosis. Front Aging Neurosci 2017;9:140.
31. Shi MC, Wang SC, Zhou HW, Xing YQ, Cheng YH, Feng JC, Wu J. Compensatory remodeling in symptomatic middle cerebral artery atherosclerotic stenosis: a high-resolution MRI and microemboli monitoring study. Neurol Res 2012;34:153-8.
32. Wang Y, Bai Y, Wang ZX, Ma XY, Wei W, Shi SJ, Wang MY. Evaluation of the relations between middle cerebral artery plaque characteristics and ischemic stroke and transient ischemic attack: three-dimensional high-resolution magnetic resonance imaging. Chinese Journal of Magnetic Resonance Imaging 2019;10:169-73.
33. Zhao DL, Deng G, Xie B, Ju S, Yang M, Chen XH, Teng GJ. High-resolution MRI of the vessel wall in patients with symptomatic atherosclerotic stenosis of the middle cerebral artery. J Clin Neurosci 2015;22:700-4.
34. Wang W, Yang Q, Li D, Fan Z, Bi X, Du X, Wu F, Wu Y, Li K. Incremental Value of Plaque Enhancement in Patients with Moderate or Severe Basilar Artery Stenosis: 3.0 T High-Resolution Magnetic Resonance Study. Biomed Res Int 2017;2017:4281629.
35. Chen Z, Liu AF, Chen H, Yuan C, He L, Zhu Y, Guan M, Jiang WJ, Zhao X. Evaluation of basilar artery atherosclerotic plaque distribution by 3D MR vessel wall imaging. J Magn Reson Imaging 2016;44:1592-9.
36. Jeong SK, Lee JH, Nam DH, Kim JT, Ha YS, Oh SY, Park SH, Lee SH, Hur N, Kwak HS, Chung GH. Basilar artery angulation in association with aging and pontine lacunar infarction: a multicenter observational study. J Atheroscler Thromb 2015;22:509-17.
37. Dieleman N, van der Kolk AG, Zwanenburg JJ, Harteveld AA, Biessels GJ, Luijten PR, Hendrikse J. Imaging intracranial vessel wall pathology with magnetic resonance imaging: current prospects and future directions. Circulation 2014;130:192-201.
38. Qiao Y, Zeiler SR, Mirbagheri S, Leigh R, Urrutia V, Wityk R, Wasserman BA. Intracranial plaque enhancement in patients with cerebrovascular events on high-spatial-resolution MR images. Radiology 2014;271:534-42.
39. Klein IF, Labreuche J, Lavallée PC, Mazighi M, Duyckaerts C, Hauw JJ, Amarenco P. Is moderate atherosclerotic stenosis in the middle cerebral artery a cause of or a coincidental finding in ischemic stroke? Cerebrovasc Dis 2010;29:140-5.
40. Kerwin WS, Oikawa M, Yuan C, Jarvik GP, Hatsukami

TS. MR imaging of adventitial vasa vasorum in carotid atherosclerosis. Magn Reson Med 2008;59:507-14.
41. Wu F, Ma Q, Song H, Guo X, Diniz MA, Song SS, Gonzalez NR, Bi X, Ji X, Li D, Yang Q, Fan Z; . Differential Features of Culprit Intracranial Atherosclerotic Lesions: A Whole-Brain Vessel Wall Imaging Study in Patients With Acute Ischemic Stroke. J Am Heart Assoc 2018;7:e009705.
42. Lee HN, Ryu CW, Yun SJ. Vessel-Wall Magnetic Resonance Imaging of Intracranial Atherosclerotic Plaque and Ischemic Stroke: A Systematic Review and Meta-Analysis. Front Neurol 2018;9:1032.
43. Del Brutto OH, Mera RM, Costa AF, Del Brutto VJ. Basilar Artery Diameter Is Inversely Associated with Fetal Type Circle of Willis. Eur Neurol 2017;78:217-20.
44. Stefanadis C, Antoniou CK, Tsiachris D, Pietri P. Coronary Atherosclerotic Vulnerable Plaque: Current Perspectives. J Am Heart Assoc 2017;6:e005543.
45. Kang HG, Lee CH, Shin BS, Chung GH, Kwak HS. Characteristics of Symptomatic Basilar Artery Stenosis Using High-Resolution Magnetic Resonance Imaging in Ischemic Stroke Patients. J Atheroscler Thromb 2021;28:1063-70.
46. Fukumoto Y, Hiro T, Fujii T, Hashimoto G, Fujimura T, Yamada J, Okamura T, Matsuzaki M. Localized elevation of shear stress is related to coronary plaque rupture: a 3-dimensional intravascular ultrasound study with in-vivo color mapping of shear stress distribution. J Am Coll Cardiol 2008;51:645-50.

Cite this article as: Liu D, Zhao C, Zhao DL, Chen XH, Zhou D, Li C. Association between the fetal-type posterior cerebral artery and intracranial anterior and posterior circulating atherosclerotic plaques using multi-contrast magnetic resonance vessel wall imaging. Quant Imaging Med Surg 2023;13(12):8383-8394. doi: 10.21037/qims-23-611

